

Error analysis of the implicit variable-step BDF2 method for the molecular beam epitaxial model with slope selection

Xuan Zhao¹, Haifeng Zhang¹ and Hong Sun^{1,2}

¹ School of Mathematics, Southeast University, Nanjing 210096, P. R. China

² Department of Mathematics and Physics, Nanjing Institute of Technology, Nanjing 211167

Abstract. We derive unconditionally stable and convergent variable-step BDF2 scheme for solving the MBE model with slope selection. The discrete orthogonal convolution kernels of the variable-step BDF2 method is commonly utilized recently for solving the phase field models. In this paper, we further prove some new inequalities, concerning the vector forms, for the kernels especially dealing with the nonlinear terms in the slope selection model. The convergence rate of the fully discrete scheme is proved to be two both in time and space in L^2 norm under the setting of the variable time steps. Energy dissipation law is proved rigorously with a modified energy by adding a small term to the discrete version of the original free energy functional. Two numerical examples including an adaptive time-stepping strategy are given to verify the convergence rate and the energy dissipation law.

AMS subject classifications: 35Q92, 65M06, 65M12, 74A50

Key words: molecular beam epitaxial growth, slope selection, variable-step BDF2 scheme, energy stability, convergence.

1. Introduction

Over the past decades, the dynamics of molecular beam epitaxy (MBE) model attracted broad interest from the fields of chemistry, material science, mathematics and etc. The epitaxial growth process offers a controllable method to obtain lateral heterojunction, with an atomically sharp interface, for some attractive materials in making smaller transistors [1,2]. Atomistic models, continuum models and hybrid models, from various scales, are applied to study the evolution of the surface morphology during epitaxial growth. MBE is the most widely used technique for growing thin epitaxial layers of semiconductor crystals and metallic materials [3]. In addition, Nair et al. [4] introduced the growth of superconducting Sr_2RuO_4 thin films by MBE on (110) $NdGaO_3$ substrates with transition temperatures of up to 1.8 K.

*Corresponding author. *Email addresses:* xuanzhao11@seu.edu.cn (X. Zhao), 220211744@seu.edu.cn (H. F. Zhang), sunhongzha1@126.com (H. Sun)

In this paper, we consider the MBE model with slope selection in the two-dimensional domain $\Omega = (0, L)^2 \subset \mathbb{R}^2$. Let $u(\mathbf{x}, t)$ be the epitaxy surface height with space variable $\mathbf{x} \in \Omega$ and time variable $t \geq 0$, the height evolution equation [5] is expressed as follows

$$u_t + \delta \Delta^2 u - \nabla \cdot f(\nabla u) = 0, \quad \mathbf{x} \in \Omega, \quad 0 < t \leq T, \quad (1.1)$$

subjected to the periodic boundary conditions and the initial data $u(\mathbf{x}, 0) = \varphi_0(\mathbf{x})$. Here, $\delta > 0$ is the constant that represents the width of the rounded corners on the otherwise faceted crystalline thin films. The vector f is the nonlinear bulk force, defined by

$$f(\mathbf{v}) = (|\mathbf{v}|^2 - 1)\mathbf{v}. \quad (1.2)$$

When $t \rightarrow \infty$, one obtains $|\nabla \phi| \rightarrow 1$, that is why it is called the model with slope selection. There is also a counterpart model, in which $f(\mathbf{v}) = -\mathbf{v}/(1+|\mathbf{v}|^2)$, called MBE model without slope selection due to that during the coarsening process $|\nabla \phi|$ does not converge to a constant. For any $u \in H^1(\Omega)$, define the energy function by

$$E(t) = \int_0^t \|u_t(\cdot, \cdot, s)\|^2 ds + \frac{\delta}{2} \|\Delta u(\cdot, \cdot, t)\|^2 + \frac{1}{4} \iint_{\Omega} (|\nabla u(x, y, t)|^2 - 1)^2 dx dy.$$

The following energy dissipation law holds

$$\frac{dE(t)}{dt} = 0, \quad t > 0.$$

The model (1.1) has been applied to modeling interfacial coarsening dynamics in epitaxial growth with slope selection, where the fourth-order term models surface diffusion, and the nonlinear second-order term models the well-known Ehrlich-Schwoebel effect, which consequently leads to the formation of mounds and pyramids on the growing surface. Gyure et al. [6] conducted an experiment to show the unstable growth of thin films on rough surfaces. The MBE of InAs buffer layers is performed on InAs(001) substrates, in the experiment, which exhibit large-small-large wavelength oscillations as the thickness of buffer layers increasing. This morphological instability in the rough-smooth-rough pattern is fundamentally due to the Ehrlich-Schwoebel effect.

The well-posedness for the growth equation with slope selection for different boundary conditions was studied in King et al. [7]. Li and Liu [8] proved the well-posedness and the solution regularity for the initial-boundary-value thin film epitaxy model. The Galerkin spectral method was applied to solve the numerical solution of the model with or without slope selection. In addition, numerical results showed the decay of energy and roughness at different time stages. Li et al. [9] analyzed the gradient flow modeling the epitaxial growth of thin films with slope selection in physical dimensions. The improved local and global well-posedness for solutions with critical regularity were established. Several lower and upper bounds for the gradient were obtained.

Due to the high order derivatives and the nonlinear term, it takes a long time to reach the steady state in the dynamics of the MBE model. As is well known that the linearized

schemes can avoid solving large nonlinear systems, whereas, the stabilized term usually needs to be added to the scheme in order to guarantee the stability of the scheme. However, the nonlinear schemes, which cause large computational cost, are usually stable. How to develop proper temporal discretization for the nonlinear term is a key issue to preserve energy stability at the time-discrete level and balance the computational cost. The splitting schemes are adequate choices for the fast simulation. Moreover, variable time-stepping methods are also proved as the efficient techniques, which are fundamentally difficult in the analysis for the long time simulation.

Existing attentions are given to apply the linearized schemes for solving the MBE models with slope selection. The linearized backward Euler difference scheme and the linearized Crank-Nicolson difference scheme were derived in [10]. Yang et al. [11] developed a first and second order time-stepping scheme based on the Invariant Energy Quadratization method, in which all nonlinear terms were treated semi-explicitly. Besides, there were also schemes that result in linear systems at each time step(cf., e.g., [12, 13]). For the MBE models without slope selection, we further refer to the monograph [14–20] on the linearized schemes. The stabilized terms are usually utilized in order to preserve the stability of the linearized schemes. Xu and Tang [21] constructed linearized schemes added with the stabilized terms, which are consistent with the orders of the time discretizations, and showed that the schemes allow much larger time steps than those of a standard implicit-explicit approach. Li et al. [22] proved the unconditional energy stability for the stabilized semi-implicit time-stepping methods without the Lipschitz assumption on the nonlinearity. Utilizing a regularized term, Chen et al. [13] proposed a fully discrete scheme, which preserves energy-dissipation property, for the MBE model with slope selection. The scaling law for the roughness growing and effective energy decaying are captured in the long time simulations. Other cases concerning the effect of the stabilized terms in solving MBE models with slope selection can be found in [23, 24]. We also refer the reader to the references therein [14–17, 25, 26] on the stabilized terms for the MBE models without slope selection.

Whereas, the nonlinear schemes are also selected for numerically solving MBE models due to its advantages in preserving stability in the long time computations. Chen and Wang [27] presented a semi-implicit nonlinear scheme which combined the mixed finite element method and the backward Euler scheme for the thin film epitaxy problem with slope selection. The mixed formulation only needs to use C^1 elements by introducing proper dual variables, which are defined naturally from the nonlinear term in the equation. Feng et al. [23] studied an implicit nonlinear finite difference scheme using two-step backward differentiation formula (BDF2) method with constant coefficient stabilizing terms for the epitaxial thin film equation with slope selection. The efficient preconditioned steepest descent and the preconditioned nonlinear conjugate gradient algorithms were applied to solve the corresponding nonlinear system. An energy stable, nonlinear mixed finite element scheme was proposed and analyzed for the thin film epitaxial growth model with slope selection [24]. An optimal convergence rate was obtained with the help of some auxiliary techniques over triangular elements. Additional theoretical frameworks for nonlinear schemes were described in [28, 29]. Furthermore, for the nonlinear schemes for the MBE model without slope selection, we refer to [25, 30, 31] and the references therein.

One approach to achieve fast simulation appropriately in the presence of the nonlinear terms in MBE model is the splitting method. Cheng et al. [32] introduced fast explicit operator splitting methods for both one- and two-dimensional nonlinear diffusion equations for thin film epitaxy with slope selection. A fast explicit operator splitting method, which splits the original problem into linear and nonlinear subproblems, was proposed for the epitaxial growth model with slope selection [33]. The convergence rate of the algorithm in discrete L^2 norm was analyzed theoretically. Lee et al. [34] developed an operator splitting Fourier spectral method, which alleviates restriction on the time steps, for epitaxial thin film growth with and without slope selection. Different forms about the splitting method for MBE model with slope selection were mentioned in [35–39]. As a supplement, we refer to [25, 40–43] for the splitting method in the MBE models without slope selection.

An efficient approach for avoiding large computational cost in the long time simulation is the adaptive technique. Qiao et al. [44] applied time adaptivity strategies for some unconditionally energy stable finite difference schemes and showed that the steady-state solutions and the dynamical changes of the solution are resolved accurately and efficiently. Luo et al. [29] developed two types of adaptive time-stepping methods in which equidistribution of the physical quantities in time direction was taken to control the simulation error. Liao et al. [45] introduced the BDF2 scheme with variable steps for the MBE model without slope selection, the L^2 norm stability and rigorous error estimates of which were established under an improved step-ratio constraint. A detailed survey on all related literature would exceed the scope of this paper. Therefore, we confine ourselves to the papers mentioned above and the references therein.

Over the last 20 years, variable contributions have delineated the numerical computations of MBE models. In the current work, we focus on the analysis of the variable-step BDF2 scheme for the model with slope selection. We have followed the analysis of variable-step BDF2 scheme for Cahn-Hilliard model in [46]. In particular, for the kernels and the time-step ratios derived in [46], we proved Lemma 3.2, Lemma 3.3 and Lemma 3.4 concerning the vector forms dealing with the nonlinear terms, for analyzing convergence properties and deriving error estimates of the proposed scheme. The unique solvability and the energy stability of the scheme is demonstrated by virtue of the properties of the convolution coefficients under the same mild time-step ratios restriction.

The rest of the paper is structured as follows. In section 2, we establish an implicit variable-step BDF2 scheme and introduce some preliminary lemmas that facilitate the unique solvability and the energy dissipation law of the difference scheme. In section 3, we introduce some fundamental properties and several discrete convolution inequalities with respect to the discrete orthogonal convolution (DOC) kernels which help demonstrating the error estimate of the proposed scheme. We perform and discuss typical numerical examples in section 4 to verify the theoretical results.

2. Discrete energy dissipation law

In this section, we investigate the unique solvability of the difference scheme (2.2) based on the Brouwer fixed-point theorem. By virtue of the properties of the convolution coeffi-

cients, the energy stability of the scheme is demonstrated. We start with the introduction of some notations.

For the spatial direction discretization, let M be a positive integer, $\Omega = (0, L)^2$ and $x_i = ih$, $y_j = jh$ with the spatial lengths $h_x = h_y = h := L/M$. Set the discrete spatial grid $\Omega_h := \{(x_i, y_j) \mid 1 \leq i, j \leq M\}$ and $\bar{\Omega}_h := \{(x_i, y_j) \mid 0 \leq i, j \leq M\}$. Consider the L -periodic function space

$$\mathbb{V}_h := \{v_h = v(x_h) \mid x_h = (x_i, y_j) \in \bar{\Omega}_h \text{ and } v_h \text{ is } L\text{-periodic in each direction}\}.$$

Given a grid function $v \in \mathbb{V}_h$, introduce the following notations $\delta_x v_{i+\frac{1}{2},j} = (v_{i+1,j} - v_{i,j})/h$, $\Delta_x v_{ij} = (v_{i+1,j} - v_{i-1,j})/(2h)$, and $\delta_x^2 v_{ij} = (\delta_x v_{i+\frac{1}{2},j} - \delta_x v_{i-\frac{1}{2},j})/h$. The discrete notations $\delta_y v_{i,j+\frac{1}{2}}$, $\Delta_y v_{ij}$ and $\delta_y^2 v_{ij}$ can be defined similarly. Also, we define the discrete Laplacian operator $\Delta_h v_{ij} = \delta_x^2 v_{ij} + \delta_y^2 v_{ij}$ and the discrete gradient vector $\nabla_h v_{ij} = (\Delta_x v_{ij}, \Delta_y v_{ij})^T$.

For any grid functions $v, w \in \mathbb{V}_h$, define the inner product $\langle v, w \rangle := h^2 \sum_{x_h \in \Omega_h} v_h w_h$, the associated L^2 norm $\|v\| := \sqrt{\langle v, v \rangle}$, and the discrete L^q norm $\|v\|_{l^q} := \sqrt[q]{h^2 \sum_{x_h \in \Omega_h} |v_h|^q}$. The discrete seminorms $\|\nabla_h v\|_{l^q}$ and $\|\Delta_h v\|_{l^q}$ are defined similarly. In addition, $\|\delta_x v\|$ and $\|\delta_y v\|$ are written as

$$\|\delta_x v\| = \sqrt{h^2 \sum_{x_h \in \Omega_h} (\delta_x v_{i-\frac{1}{2},j})^2}, \quad \|\delta_y v\| = \sqrt{h^2 \sum_{x_h \in \Omega_h} (\delta_y v_{i,j-\frac{1}{2}})^2}.$$

The discrete H^1 -seminorm is defined by $|v|_1 = \sqrt{\|\delta_x v\|^2 + \|\delta_y v\|^2}$. Furthermore, the discrete Green's formula with periodic boundary conditions yield $\langle \Delta_h^2 v, w \rangle = \langle \Delta_h v, \Delta_h w \rangle$ and $-\langle \nabla_h \cdot \nabla_h v, w \rangle = \langle \nabla_h v, \nabla_h w \rangle$. In the subsequent analysis, we need the commonly used discrete Sobolev embedding inequality

$$\|\nabla_h v\|^2 \leq \|\Delta_h v\| \cdot \|v\|. \quad (2.1)$$

For the time discretization, take time levels $0 = t_0 < t_1 < t_2 < \dots < t_N = T$ with the time-step $\tau_n = t_n - t_{n-1}$ for $1 \leq n \leq N$. Let the adjacent time-step ratios $r_n := \tau_n / \tau_{n-1}$ for $2 \leq n \leq N$. For any grid function $v^n = v(t_n)$, we denote $\nabla_\tau v^n := v^n - v^{n-1}$ and $\partial_\tau v^n := \nabla_\tau v^n / \tau_n$. The well-known variable-step BDF2 formula reads

$$D_2 v^n := \frac{1 + 2r_n}{\tau_n(1 + r_n)} \nabla_\tau v^n - \frac{r_n^2}{\tau_n(1 + r_n)} \nabla_\tau v^{n-1} \quad \text{for } n \geq 2.$$

Always, one needs a starting scheme to compute the first-level solution v^1 since the two-step BDF2 formula needs two starting values. To improve the temporal accuracy at the time $t = t_1$, we adopt a second-order accurate approach

$$D_2 v^1 := \frac{2}{\tau_1} \left[v^1 - \left(v(t_0) + \frac{\tau_1}{2} v_t(t_0) \right) \right]$$

using the fact that $\frac{1}{2}[v_t(t_1) + v_t(t_0)] = \frac{1}{\tau_1}(v^1 - v(t_0)) + O(\tau_1^2)$.

We give the implicit variable-step BDF2 scheme for the MBE problem (1.1) as

$$D_2 u_h^n + \delta \Delta_h^2 u_h^n - \nabla_h \cdot f(\nabla_h u_h^n) = 0 \quad \text{for } x_h \in \Omega_h, 1 \leq n \leq N \quad (2.2)$$

with the initial data $u_h^0 = \varphi_0(x_h) - \frac{\tau_1}{2} \varphi_1(x_h)$ for $x_h \in \bar{\Omega}_h$, where $\varphi_1 := \nabla \cdot f(\nabla \varphi_0) - \delta \Delta^2 \varphi_0$ for the smooth data $\varphi_0 \in H^4(\Omega)$. The spatial operators are approximated by the finite difference method. We start our analysis by viewing the above BDF2 formula as a discrete convolution summation $D_2 v^n := \sum_{k=1}^n b_{n-k}^{(n)} \nabla_\tau v^k$ for $n \geq 1$, where the discrete convolution kernels $b_{n-k}^{(n)}$ are defined by $b_0^{(1)} := 2/\tau_1$, and when $n \geq 2$,

$$b_0^{(n)} := \frac{1 + 2r_n}{\tau_n(1 + r_n)}, \quad b_1^{(n)} := -\frac{r_n^2}{\tau_n(1 + r_n)} \quad \text{and} \quad b_j^{(n)} := 0 \quad \text{for } 2 \leq j \leq n-1. \quad (2.3)$$

The variable-step BDF2 time-stepping was considered recently in [46, 47] from a new point of view by making the virtue of the positive definiteness of BDF2 convolution kernels $b_{n-k}^{(n)}$. A concise L^2 norm stability and convergence theory of variable-step BDF2 scheme has been established for the linear diffusion equations provided that the adjacent time-step ratios $r_k \leq r_s < 4.864$ for $2 \leq k \leq N$. The discrete tool as a counterpart is the so-called DOC kernels, given by

$$\theta_0^{(n)} := \frac{1}{b_0^{(n)}} \quad \text{and} \quad \theta_{n-k}^{(n)} := -\frac{1}{b_0^{(k)}} \sum_{j=k+1}^n \theta_{n-j}^{(n)} b_{j-k}^{(j)} \quad \text{for } 1 \leq k \leq n-1, \quad (2.4)$$

deduced by the following discrete orthogonal identity

$$\sum_{j=k}^n \theta_{n-j}^{(n)} b_{j-k}^{(j)} \equiv \delta_{nk} \quad \text{for } 1 \leq k \leq n, \quad (2.5)$$

where δ_{nk} is the Kronecker delta symbol. By exchanging the summation order and using the identity (2.5), it is not difficult to check that

$$\sum_{j=1}^n \theta_{n-j}^{(n)} D_2 v^j = \nabla_\tau v^n \quad \text{for } \{v^j \mid 0 \leq j \leq n\}. \quad (2.6)$$

This equality (2.6) will play an important role in the subsequent analysis. The detailed properties of the DOC kernels $\theta_{n-k}^{(n)}$ are referred to Lemma 3.1. Lemma 2.2 shows that the BDF2 convolution kernels $b_{n-k}^{(n)}$ are positive definite provided the adjacent time-step ratios r_k satisfy a sufficient condition $r_k \leq r_s$ for $2 \leq k \leq N$.

2.1. Unique solvability

To prove the unique solvability, we need the following lemma.

Lemma 2.1. For any vectors \mathbf{u} , \mathbf{v} and $\mathbf{z} := \mathbf{u} - \mathbf{v}$, it holds that

$$\begin{aligned} (\mathbf{u} - \mathbf{v})^T f(\mathbf{u}) &\geq \frac{1}{4}(|\mathbf{u}|^4 - |\mathbf{v}|^4) - \frac{1}{2}(|\mathbf{u}|^2 - |\mathbf{v}|^2) - \frac{1}{2}|\mathbf{u} - \mathbf{v}|^2, \\ \mathbf{z}^T [f(\mathbf{u}) - f(\mathbf{v})] &\geq \frac{1}{2}|\mathbf{v}|^2|\mathbf{z}|^2 + \frac{1}{2}(\mathbf{u}^T \mathbf{z})^2 - |\mathbf{z}|^2. \end{aligned}$$

Proof. We observe the fact that $\mathbf{u}^T(\mathbf{u} - \mathbf{v}) = \frac{1}{2}(|\mathbf{u}|^2 - |\mathbf{v}|^2 + |\mathbf{u} - \mathbf{v}|^2)$, it follows by omitting the nonnegative term $|\mathbf{u}|^2|\mathbf{u} - \mathbf{v}|^2$ and the mean value inequality

$$\begin{aligned} (\mathbf{u} - \mathbf{v})^T f(\mathbf{u}) &= (|\mathbf{u}|^2 - 1)\mathbf{u}^T(\mathbf{u} - \mathbf{v}) \\ &= \frac{1}{2}(|\mathbf{u}|^2 - 1)(|\mathbf{u}|^2 - |\mathbf{v}|^2 + |\mathbf{u} - \mathbf{v}|^2) \\ &\geq \frac{1}{4}(|\mathbf{u}|^4 - |\mathbf{v}|^4) - \frac{1}{2}(|\mathbf{u}|^2 - |\mathbf{v}|^2) - \frac{1}{2}|\mathbf{u} - \mathbf{v}|^2. \end{aligned}$$

It follows from Young's inequality that

$$\begin{aligned} \mathbf{z}^T [f(\mathbf{u}) - f(\mathbf{v})] &= [|\mathbf{u}|^2 \mathbf{u} - |\mathbf{v}|^2 \mathbf{v} - \mathbf{z}]^T \mathbf{z} \\ &= [(|\mathbf{u}|^2 - |\mathbf{v}|^2)\mathbf{u} + |\mathbf{v}|^2 \mathbf{z}]^T \mathbf{z} - |\mathbf{z}|^2 \\ &= [(\mathbf{u}^T \mathbf{z} + \mathbf{v}^T \mathbf{z})\mathbf{u}]^T \mathbf{z} + |\mathbf{v}|^2 |\mathbf{z}|^2 - |\mathbf{z}|^2 \\ &= |\mathbf{v}|^2 |\mathbf{z}|^2 + (\mathbf{u}^T \mathbf{z} + \mathbf{v}^T \mathbf{z})\mathbf{u}^T \mathbf{z} - |\mathbf{z}|^2 \\ &\geq \frac{1}{2}|\mathbf{v}|^2 |\mathbf{z}|^2 + \frac{1}{2}(\mathbf{u}^T \mathbf{z})^2 - |\mathbf{z}|^2. \end{aligned}$$

This completes the proof.

Theorem 2.1. Suppose the time-step ratios satisfy $r_k \leq r_s$ for $2 \leq k \leq N$ and the time-step size $\tau_n < \frac{4\delta(1+2r_n)}{1+r_n}$ for $1 \leq n \leq N$. The difference scheme (2.2) is uniquely solvable.

Proof. The Brouwer fixed-point theorem is applied to show the solvability of the difference scheme (2.2). For any fixed index $n \geq 1$, we construct the map $\Pi_n : \mathbb{V}_h \rightarrow \mathbb{V}_h$ as follows

$$\Pi_n(w_h) := b_0^{(n)} w_h - g_h^{n-1} + \delta \Delta_h^2 w_h - \nabla_h \cdot f(\nabla_h w_h), \quad \mathbf{x}_h \in \bar{\Omega}_h. \quad (2.7)$$

where $g_h^{n-1} = b_0^{(n)} u_h^{n-1} - b_1^{(n)} \nabla_\tau u_h^{n-1}$, for $n \geq 2$ and $g_h^0 = b_0^{(1)} u_h^0$.

Suppose u^{n-1} , u^{n-2} have been determined, taking the inner product of $\Pi_n(w)$ with w , it yields

$$\langle \Pi_n(w), w \rangle = b_0^{(n)} \langle w, w \rangle + \delta \langle \Delta_h^2 w, w \rangle - \langle \nabla_h \cdot f(\nabla_h w), w \rangle - \langle g^{n-1}, w \rangle.$$

Combining the embedding inequality (2.1) and Young's inequality, it follows that

$$\begin{aligned} \langle \Pi_n(w), w \rangle &\geq b_0^{(n)} \|w\|^2 + \delta \|\Delta_h w\|^2 + \|\nabla_h w\|_{L^4}^4 - \|\nabla_h w\|^2 - \|g^{n-1}\| \cdot \|w\| \\ &\geq b_0^{(n)} \|w\|^2 + \delta \|\Delta_h w\|^2 - (\delta \|\Delta_h w\|^2 + \frac{1}{4\delta} \|w\|^2) - \|g^{n-1}\| \cdot \|w\| \\ &= (b_0^{(n)} - \frac{1}{4\delta}) \|w\|^2 - \|g^{n-1}\| \cdot \|w\|. \end{aligned}$$

When $\tau_n < \frac{4\delta(1+2r_n)}{1+r_n}$ and $\|w\| = 4\delta\|g^{n-1}\|/(4\delta b_0^{(n)} - 1)$, we arrive at

$$\langle \Pi_n(w), w \rangle \geq 0.$$

With the help of the Brouwer fixed-point theorem, there exists a w_h^* such that $\Pi_n(w_h^*) = 0$ which implies that the variable-step BDF2 scheme (2.2) is solvable.

Next, we show the uniqueness of the solutions. Suppose both w_h and v_h are the solutions of the difference scheme (2.2). Denote the difference $\rho_h = w_h - v_h$. Then it follows that

$$b_0^{(n)}\rho_h + \delta\Delta_h^2\rho_h - \nabla_h \cdot (f(\nabla_h w_h) - f(\nabla_h v_h)) = 0. \quad (2.8)$$

Taking the inner product of (2.8) with ρ , we have

$$b_0^{(n)}\|\rho\|^2 + \delta\|\Delta_h\rho\|^2 + \langle f(\nabla_h w) - f(\nabla_h v), \nabla_h\rho \rangle = 0.$$

Making use of Lemma 2.1 and taking $\mathbf{u} = \nabla_h u$, $\mathbf{v} = \nabla_h v$ and $\mathbf{z} = \nabla_h\rho$, it yields

$$b_0^{(n)}\|\rho\|^2 + \delta\|\Delta_h\rho\|^2 + \frac{1}{2}h^2 \sum_{\mathbf{x}_h \in \Omega_h} (|\nabla_h v_h|^2 |\nabla_h\rho_h|^2 + (\nabla_h u_h \cdot \nabla_h\rho_h)^2) \leq \|\nabla_h\rho\|^2.$$

Noticing that the third term on the left hand side is nonnegative, with the help of the embedding inequality (2.1), we have

$$b_0^{(n)}\|\rho\|^2 + \delta\|\Delta_h\rho\|^2 \leq \delta\|\Delta_h\rho\|^2 + \frac{1}{4\delta}\|\rho\|^2.$$

When $\tau_n < \frac{4\delta(1+2r_n)}{1+r_n}$, the above inequality implies that $\|\rho\| = 0$. This completes the proof.

2.2. Energy dissipation law

Now we present the energy stability of the scheme (2.2). The following lemma shows the convolution kernels $b_{n-k}^{(n)}$ are positive definite if the time-step ratios satisfy $r_k \leq r_s$ for $2 \leq k \leq N$.

Lemma 2.2. [46] *Let the time-step ratios satisfy $r_k \leq r_s$ for $2 \leq k \leq N$, for any real sequence $\{w^k\}_{k=1}^n$ with n entries, it holds that*

$$2w_k \sum_{j=1}^k b_{k-j}^{(k)} w_j \geq \frac{r_{k+1}^{\frac{3}{2}}}{1+r_{k+1}} \frac{w_k^2}{\tau_k} - \frac{r_k^{\frac{3}{2}}}{1+r_k} \frac{w_{k-1}^2}{\tau_{k-1}} + R_L(r_k, r_{k+1}) \frac{w_k^2}{\tau_k} \quad \text{for } k \geq 2,$$

where $R_L(z, s) = \frac{2+4z-z^{\frac{3}{2}}}{1+z} - \frac{s^{\frac{3}{2}}}{1+s}$, $0 < z, s < r_s$. Thus the discrete convolution kernels $b_{n-k}^{(n)}$ are positive definite

$$\sum_{k=1}^n w_k \sum_{j=1}^k b_{k-j}^{(k)} w_j \geq \frac{1}{2} \sum_{k=1}^n R_L(r_k, r_{k+1}) \frac{w_k^2}{\tau_k} \quad \text{for } n \geq 1.$$

We define the discrete energy $E^n = \frac{\delta}{2} \|\Delta_h u^n\|^2 + \frac{1}{4} \|\ |\nabla_h u^n|^2 - 1 \|^2$, for $n \geq 0$. Furthermore, the modified discrete energy is defined by $\mathcal{E}^n = E^n + \frac{r_{n+1}^{\frac{3}{2}}}{2(1+r_{n+1})\tau_n} \|\nabla_\tau u^n\|^2$, for $n \geq 1$, with $\mathcal{E}^0 = E^0$.

Theorem 2.2. *If the time-step ratios satisfy $r_k \leq r_s$ for $2 \leq k \leq N$ and the time-step size*

$$\tau_n < 4\delta \min \left\{ R_L(r_n, r_{n+1}), \frac{2+r_2}{1+r_2} \right\}, \quad (2.9)$$

then the solution of the variable-step BDF2 scheme (2.2) satisfies

$$E^n \leq \mathcal{E}^n \leq \mathcal{E}^{n-1} \leq E^0, \quad 1 \leq n \leq N.$$

Proof. We start our proof by taking the inner product of (2.2) with $\nabla_\tau u^n$, it yields

$$\langle D_2 u^n, \nabla_\tau u^n \rangle + \delta \langle \Delta_h^2 u^n, \nabla_\tau u^n \rangle - \langle \nabla_h \cdot f(\nabla_h u^n), \nabla_\tau u^n \rangle = 0. \quad (2.10)$$

For $n \geq 2$, taking $w_n = \nabla_\tau u^n$ in the first inequality of Lemma 2.2, we obtain an estimate of the first term on the left hand in (2.10),

$$\begin{aligned} \langle D_2 u^n, \nabla_\tau u^n \rangle &\geq \frac{r_{n+1}^{\frac{3}{2}}}{2(1+r_{n+1})\tau_n} \|\nabla_\tau u^n\|^2 - \frac{r_n^{\frac{3}{2}}}{2(1+r_n)\tau_{n-1}} \|\nabla_\tau u^{n-1}\|^2 \\ &\quad + \frac{1}{2\tau_n} R_L(r_n, r_{n+1}) \|\nabla_\tau u^n\|^2. \end{aligned}$$

By virtue of the summation by parts and the equality $2a(a-b) = a^2 - b^2 + (a-b)^2$, we have the diffusion term rewritten as

$$\langle \Delta_h^2 u^n, \nabla_\tau u^n \rangle = \frac{1}{2} (\|\Delta_h u^n\|^2 - \|\Delta_h u^{n-1}\|^2 + \|\Delta_h(\nabla_\tau u^n)\|^2).$$

An application of Lemma 2.1 with $\mathbf{u} = \nabla_h u^n$ and $\mathbf{v} = \nabla_h u^{n-1}$ gives an lower bound of the nonlinear part

$$\begin{aligned} -\langle \nabla_h \cdot f(\nabla_h u^n), \nabla_\tau u^n \rangle &= \langle f(\nabla_h u^n), \nabla_\tau(\nabla_h u^n) \rangle \\ &\geq \frac{1}{4} (\|\nabla_h u^n\|_{l^4}^4 - \|\nabla_h u^{n-1}\|_{l^4}^4) - \frac{1}{2} (\|\nabla_h u^n\|^2 - \|\nabla_h u^{n-1}\|^2) - \frac{1}{2} \|\nabla_h(\nabla_\tau u^n)\|^2 \\ &\geq \frac{1}{4} \|\ |\nabla_h u^n|^2 - 1 \|^2 - \frac{1}{4} \|\ |\nabla_h u^{n-1}|^2 - 1 \|^2 - \frac{1}{2} \|\nabla_h(\nabla_\tau u^n)\|^2. \end{aligned}$$

Substituting the above treatments into (2.10), the modified discrete energy \mathcal{E}^n is given in the whole inequality

$$\begin{aligned} &\mathcal{E}^n + \frac{1}{2\tau_n} R_L(r_n, r_{n+1}) \|\nabla_\tau u^n\|^2 + \frac{\delta}{2} \|\Delta_h(\nabla_\tau u^n)\|^2 \\ &\leq \mathcal{E}^{n-1} + \frac{1}{2} \|\nabla_h(\nabla_\tau u^n)\|^2 \\ &\leq \mathcal{E}^{n-1} + \frac{\delta}{2} \|\Delta_h(\nabla_\tau u^n)\|^2 + \frac{1}{8\delta} \|\nabla_\tau u^n\|^2, \quad 2 \leq n \leq N, \end{aligned}$$

in which the embedding inequality (2.1) is utilized. Afterwards it follows from (2.9) that $\mathcal{E}^n \leq \mathcal{E}^{n-1}$, $2 \leq n \leq N$. For $n = 1$, by Young's inequality, it yields

$$\langle D_2 u^1, \nabla_\tau u^1 \rangle \geq \frac{r_2}{2(1+r_2)\tau_1} \|\nabla_\tau u^1\|^2 + \frac{2+r_2}{2(1+r_2)\tau_1} \|\nabla_\tau u^1\|^2.$$

Then, when $\tau_1 < \frac{4\delta(2+r_2)}{1+r_2}$, we have $\mathcal{E}^1 \leq \mathcal{E}^0$. Thus, it is obvious that $E^n \leq \mathcal{E}^n \leq \mathcal{E}^0 = E^0$.

Lemma 2.3. *If the time-step ratios satisfy $r_k \leq r_s$ for $2 \leq k \leq N$ and the condition (2.9) holds, the numerical solution of the variable-step BDF2 scheme (2.2) satisfies*

$$\max\{\|\nabla_h u^n\|, \|\nabla_h u^n\|_{l^4}, \|\Delta_h u^n\|\} \leq C_0,$$

where C_0 is a constant, which is independent of the spatial lengths h and the time steps τ_n .

Proof. Using the fact that $a^4 \geq 4a^2 - 4$ and applying Theorem 2.2, it follows that

$$\begin{aligned} 4E^0 &\geq 4E^n = 2\delta\|\Delta_h u^n\|^2 + \|\nabla_h u^n\|_{l^4}^4 - 2\|\nabla_h u^n\|^2 + |\Omega_h| \\ &\geq 2\delta\|\Delta_h u^n\|^2 + \frac{1}{4}\|\nabla_h u^n\|_{l^4}^4 + \frac{3}{4}(4\|\nabla_h u^n\|^2 - 4|\Omega_h|) - 2\|\nabla_h u^n\|^2 + |\Omega_h| \\ &\geq 2\delta\|\Delta_h u^n\|^2 + \frac{1}{4}\|\nabla_h u^n\|_{l^4}^4 + \|\nabla_h u^n\|^2 - 2|\Omega_h|. \end{aligned}$$

Taking $K_0 = \min\{2\delta, 1/4\}$, we get

$$\|\Delta_h u^n\|^2 + \|\nabla_h u^n\|_{l^4}^4 + \|\nabla_h u^n\|^2 \leq (4E^0 + 2|\Omega_h|)/K_0 =: K_1.$$

Then, the desired estimate is obtained with $C_0 = \max\{\sqrt{K_1}, \sqrt[4]{K_1}\}$.

3. Convergence analysis

In this section, we derive the error estimate of the implicit variable-step BDF2 scheme (2.2). We begin with some fundamental properties and several discrete convolution inequalities with respect to the DOC kernels. For convenience, we firstly introduce the denotation

$$\sum_{k,l}^{n,k} := \sum_{k=1}^n \sum_{l=1}^k.$$

Lemma 3.1. [47] *If the discrete convolution kernels $b_{n-k}^{(n)}$ defined in (2.3) are positive definite, then the DOC kernels $\theta_{n-l}^{(n)}$ defined in (2.4) satisfy:*

(I) *The discrete kernels $\theta_{n-l}^{(n)}$ are positive definite;*

(II) $\sum_{l=1}^n \theta_{n-l}^{(n)} \leq \tau_n$ such that $\sum_{k,l}^{n,k} \theta_{k-l}^{(k)} \leq t_n$ for $n \geq 1$.

The following three lemmas are the key to proving the convergence of the BDF2 scheme (2.2) for dealing with the nonlinear term. We describe the lemmas in detail below but put their proofs to the Appendix for brief.

Lemma 3.2. *Assuming that the time-step ratios satisfy $r_k \leq r_s$ for $2 \leq k \leq N$, for any vector sequence $\{\mathbf{v}^k\}_{k=1}^n \in \mathbb{R}^2$, the following inequality holds*

$$\frac{m_1}{2m_2} \sum_{k=1}^n \tau_k (\mathbf{v}^k)^T \mathbf{v}^k \leq \sum_{k,l}^{n,k} \theta_{k-l}^{(k)} (\mathbf{v}^l)^T \mathbf{v}^k \leq \frac{m_3}{2} \sum_{k=1}^n \tau_k (\mathbf{v}^k)^T \mathbf{v}^k,$$

where m_1, m_2, m_3 are positive constants.

Lemma 3.3. *If the time-step ratios satisfy $r_k \leq r_s$ for $2 \leq k \leq N$, for any vector sequences $\{\mathbf{v}^k, \mathbf{w}^k\}_{k=1}^n$, where $\mathbf{v}^k, \mathbf{w}^k \in \mathbb{R}^2$, it holds that*

$$\sum_{k,l}^{n,k} \theta_{k-l}^{(k)} (\mathbf{v}^l)^T \mathbf{w}^k \leq \epsilon \sum_{k=1}^n \tau_k (\mathbf{v}^k)^T \mathbf{v}^k + \frac{m_3}{4m_1\epsilon} \sum_{k=1}^n \tau_k (\mathbf{w}^k)^T \mathbf{w}^k \quad \text{for } \forall \epsilon > 0.$$

Lemma 3.4. *Assume that the time-step ratios satisfy $r_k \leq r_s$ for $2 \leq k \leq N$, consider the grid function u^k and any vector sequences $\{\mathbf{z}^k, \mathbf{w}^k\}_{k=1}^n$, where $\mathbf{z}^k, \mathbf{w}^k \in \mathbb{R}^2$, and there exists a constant C_u such that*

$$C_u = \max_{1 \leq j \leq n} \|u^j\|_{l^3}.$$

Then it holds that

$$\sum_{k,l}^{n,k} \theta_{k-l}^{(k)} \langle u^l \mathbf{z}^l, \mathbf{w}^k \rangle \leq \epsilon \sum_{k=1}^n \tau_k (\|\nabla_h \mathbf{z}^k\|^2 + \|\mathbf{z}^k\|^2) + \frac{C_\Omega C_u^2 m_3}{4m_1 \epsilon} \sum_{k=1}^n \tau_k \|\mathbf{w}^k\|^2.$$

The following embedding inequalities on $\|\nabla_h v\|_{l^4}$ and $\|\nabla_h v\|_{l^6}$ are used to control the norms in the convergence analysis of the BDF2 scheme (2.2).

Lemma 3.5. *For the grid functions $v_h \in \mathbb{V}_h$, $x_h \in \Omega_h$, it holds that*

$$\|\nabla_h v\|_{l^4} \leq K_1 \|\nabla_h v\|^{\frac{1}{2}} \left(2\|\Delta_h v\|^2 + \frac{1}{L^2} \|\nabla_h v\|^2 \right)^{\frac{1}{4}} \quad (3.1)$$

and

$$\|\nabla_h v\|_{l^6} \leq K_2 \|\nabla_h v\|^{\frac{1}{3}} \left(16\|\Delta_h v\|^2 + \frac{1}{L^2} \|\nabla_h v\|^2 \right)^{\frac{1}{3}}, \quad (3.2)$$

where K_1 and K_2 are two constants.

By virtue of Lemma 2.3 and Lemma 3.5, there exists a constant K such that

$$\|\nabla_h u^n\|_{l^6} \leq K. \quad (3.3)$$

Now we present the error behavior of BDF2 time-stepping with respect to the variation of time-step sizes with the following two lemmas.

Lemma 3.6. [47] For the consistency error $\xi^j = D_2u(t_j) - \partial_t u(t_j)$ at $t = t_j$, Let P^k be a convolutional consistency error, defined by $P^k := \sum_{j=1}^k \theta_{k-j}^{(k)} \xi^j$. If the time-step ratios satisfy $r_k \leq r_s$ for $2 \leq k \leq N$, the convolutional consistency error P^k satisfies

$$\sum_{k=1}^n |P^k| \leq 3t_n \max_{1 \leq j \leq n} \left(\tau_j \int_{t_{j-1}}^{t_j} |u'''(s)| ds \right) \quad \text{for } 2 \leq n \leq N.$$

Lemma 3.7. [47] Let $\lambda \geq 0$, the sequences $\{\xi_j\}_{j=0}^N$ and $\{V_j\}_{j=1}^N$ be nonnegative. If

$$V_n \leq \lambda \sum_{j=1}^{n-1} \tau_j V_j + \sum_{j=1}^n \xi_j \quad \text{for } 1 \leq n \leq N,$$

then it holds that

$$V_n \leq \exp(\lambda t_{n-1}) \sum_{j=1}^n \xi_j \quad \text{for } 1 \leq n \leq N.$$

Now, we set about to demonstrate the convergence of the variable-step BDF2 scheme (2.2). Let $C_1 = \max_{(x,y,t) \in \Omega \times [0,T]} \{|u(x,y,t)|, |\nabla u(x,y,t)|, |\Delta u(x,y,t)|\}$. Denoting that $e_h^n = U_h^n - u_h^n$, $x_h \in \bar{\Omega}_h$, $0 \leq n \leq N$, we get the error equation as follows

$$D_2 e_h^n + \delta \Delta_h^2 e_h^n - \nabla_h \cdot (f(\nabla_h U_h^n) - f(\nabla_h u_h^n)) = \xi_h^n + \eta_h^n, \quad x_h^n \in \Omega_h, \quad 1 \leq n \leq N, \quad (3.4)$$

where ξ_h^n , η_h^n denote the local consistency error in time and space.

Theorem 3.1. Suppose the problem (1.1) has a unique smooth solution and $u_h^n \in \mathbb{V}_h$ is the solution of the difference scheme (2.2). If the time-step ratios satisfy $r_k \leq r_s$ for $2 \leq k \leq N$ with the maximum time-step size $\tau \leq \tau_0$, where τ_0 is a constant, the variable-step BDF2 scheme (2.2) is convergent in L^2 norm.

$$\|e^n\| \leq C(\tau^2 + h^2), \quad 1 \leq n \leq N.$$

Proof. Replacing n by l in (3.4), multiplying both sides of (3.4) by the DOC kernels $\theta_{k-l}^{(k)}$ and summing l from 1 to k , then it yields

$$\sum_{l=1}^k \theta_{k-l}^{(k)} D_2 e_h^l + \delta \sum_{l=1}^k \theta_{k-l}^{(k)} \Delta_h^2 e_h^l - \sum_{l=1}^k \theta_{k-l}^{(k)} \nabla_h \cdot (f(\nabla_h U_h^l) - f(\nabla_h u_h^l)) = \sum_{l=1}^k \theta_{k-l}^{(k)} (\xi_h^l + \eta_h^l). \quad (3.5)$$

Taking the inner product of (3.5) with e^k and summing k from 1 to n , we get

$$\begin{aligned} & \sum_{k,l}^{n,k} \langle \theta_{k-l}^{(k)} D_2 e^l, e^k \rangle + \delta \sum_{k,l}^{n,k} \theta_{k-l}^{(k)} \langle \Delta_h^2 e^l, e^k \rangle + \sum_{k,l}^{n,k} \theta_{k-l}^{(k)} \langle f(\nabla_h U^l) - f(\nabla_h u^l), \nabla_h e^k \rangle \\ &= \sum_{k,l}^{n,k} \theta_{k-l}^{(k)} \langle \xi^l + \eta^l, e^k \rangle. \end{aligned} \quad (3.6)$$

Noticing equality (2.6) dealing with the BDF2 discretization, we have the equality $\sum_{l=1}^k \theta_{k-l}^{(k)} D_2 e_h^l = \nabla_\tau e_h^k$. Making use of the equality $a(a-b) = \frac{1}{2}[a^2 - b^2 + (a-b)^2]$, the following result holds for the first term on the left hand side of (3.6)

$$\sum_{k=1}^n \langle \nabla_\tau e^k, e^k \rangle = \frac{1}{2} (\|e^n\|^2 - \|e^0\|^2) + \frac{1}{2} \sum_{k=1}^n \|\nabla_\tau e^k\|^2. \quad (3.7)$$

By using the summation by parts and Lemma 3.2, the diffusion term yields

$$\sum_{k,l}^{n,k} \theta_{k-l}^{(k)} \langle \Delta_h^2 e^l, e^k \rangle = \sum_{k,l}^{n,k} \theta_{k-l}^{(k)} \langle \Delta_h e^l, \Delta_h e^k \rangle \geq \frac{m_1}{2m_2} \sum_{k=1}^n \tau_k \|\Delta_h e^k\|^2. \quad (3.8)$$

For the nonlinear term, using the identity

$$\begin{aligned} f(\nabla_h U_h^l) - f(\nabla_h u_h^l) &= |\nabla_h U_h^l|^2 \nabla_h e_h^l + (|\nabla_h U_h^l|^2 - |\nabla_h u_h^l|^2) \nabla_h u_h^l - \nabla_h e_h^l \\ &= |\nabla_h U_h^l|^2 \nabla_h e_h^l + (\nabla_h U_h^l \cdot \nabla_h e_h^l + \nabla_h e_h^l \cdot \nabla_h u_h^l) \nabla_h u_h^l - \nabla_h e_h^l, \end{aligned} \quad (3.9)$$

then, it follows that

$$\begin{aligned} & \sum_{k,l}^{n,k} \theta_{k-l}^{(k)} \langle f(\nabla_h U^l) - f(\nabla_h u^l), \nabla_h e^k \rangle \\ &= \sum_{k,l}^{n,k} \theta_{k-l}^{(k)} \langle |\nabla_h U^l|^2 \nabla_h e^l, \nabla_h e^k \rangle + \sum_{k,l}^{n,k} \theta_{k-l}^{(k)} \langle (\nabla_h U^l \cdot \nabla_h e^l) \nabla_h u^l, \nabla_h e^k \rangle \\ & \quad + \sum_{k,l}^{n,k} \theta_{k-l}^{(k)} \langle (\nabla_h u^l \cdot \nabla_h e^l) \nabla_h u^l, \nabla_h e^k \rangle - \sum_{k,l}^{n,k} \theta_{k-l}^{(k)} \langle \nabla_h e^l, \nabla_h e^k \rangle. \end{aligned} \quad (3.10)$$

Next, we estimate each term on the right hand in the above equality. For the first term on the right hand in (3.10), Noticing $\| |\nabla_h U^l|^2 \|_{l^3} \leq C_1^4 |\Omega|^{\frac{2}{3}} := C_2$, and with the help of Lemma 3.4, we obtain the following inequality for any $\varepsilon_1 > 0$

$$\sum_{k,l}^{n,k} \theta_{k-l}^{(k)} \langle |\nabla_h U^l|^2 \nabla_h e^l, \nabla_h e^k \rangle \leq \varepsilon_1 \sum_{k=1}^n \tau_k (\|\Delta_h e^k\|^2 + \|\nabla_h e^k\|^2) + \frac{C_\Omega C_2^2 m_3}{4m_1 \varepsilon_1} \sum_{k=1}^n \tau_k \|\nabla_h e^k\|^2. \quad (3.11)$$

Making direct use of Lemma 3.3, one arrives the following estimate for the second term on the right hand in (3.10)

$$\begin{aligned} & \sum_{k,l}^{n,k} \theta_{k-l}^{(k)} \langle (\nabla_h U^l \cdot \nabla_h e^l) \nabla_h u^l, \nabla_h e^k \rangle \\ & \leq \varepsilon_1 \sum_{k=1}^n \tau_k \|(\nabla_h U^k \cdot \nabla_h e^k) \nabla_h u^k\|^2 + \frac{m_3}{4m_1 \varepsilon_1} \sum_{k=1}^n \tau_k \|\nabla_h e^k\|^2. \end{aligned} \quad (3.12)$$

By virtue of Cauchy-Schwarz inequality, Lemma 2.3 and the inequality (3.1), the following estimate holds for the first term on the right hand side of the above inequality

$$\begin{aligned}
\|(\nabla_h U^k \cdot \nabla_h e^k) \nabla_h u^k\|^2 &\leq h^2 \sum_{x_h \in \Omega_h} |\nabla_h U_h^k|^2 |\nabla_h e_h^k|^2 |\nabla_h u_h^k|^2 \\
&= C_1^2 \|\nabla_h u^k\|_{l^4}^2 \cdot \|\nabla_h e^k\|_{l^4}^2 \\
&\leq C_0^2 C_1^2 K_1^2 \|\nabla_h e^k\| \left(2\|\Delta_h e^k\|^2 + \frac{1}{L^2} \|\nabla_h e^k\|^2 \right)^{\frac{1}{2}} \\
&\leq C_3 (\|\nabla_h e^k\|^2 + \|\Delta_h e^k\|^2),
\end{aligned}$$

where $C_3 = C_0^2 C_1^2 K_1^2 \max\{\frac{1}{2} + \frac{1}{2L^2}, 1\}$. Then, substituting the above inequality into (3.12), it yields the final estimate of the second term on the right hand in (3.10)

$$\begin{aligned}
&\sum_{k,l}^{n,k} \theta_{k-l}^{(k)} \langle (\nabla_h U^l \cdot \nabla_h e^l) \nabla_h u^l, \nabla_h e^k \rangle \\
&\leq C_3 \varepsilon_1 \sum_{k=1}^n \tau_k (\|\nabla_h e^k\|^2 + \|\Delta_h e^k\|^2) + \frac{m_3}{4m_1 \varepsilon_1} \sum_{k=1}^n \tau_k \|\nabla_h e^k\|^2. \tag{3.13}
\end{aligned}$$

For the third term on the right hand in (3.10), by virtue of Lemma 3.3, it is easily obtained that

$$\begin{aligned}
&\sum_{k,l}^{n,k} \theta_{k-l}^{(k)} \langle (\nabla_h u^l \cdot \nabla_h e^l) \nabla_h u^l, \nabla_h e^k \rangle \\
&\leq \varepsilon_1 \sum_{k=1}^n \tau_k \left\| (\nabla_h u^k \cdot \nabla_h e^k) \nabla_h u^k \right\|^2 + \frac{m_3}{4m_1 \varepsilon_1} \sum_{k=1}^n \tau_k \|\nabla_h e^k\|^2. \tag{3.14}
\end{aligned}$$

Making use of Cauchy-Schwarz inequality, it follows from (3.3) and (3.2) that

$$\begin{aligned}
\left\| (\nabla_h u^k \cdot \nabla_h e^k) \nabla_h u^k \right\|^2 &\leq h^2 \sum_{x_h \in \Omega_h} |\nabla_h u_h^k|^4 |\nabla_h e_h^k|^2 \\
&\leq K^4 \|\nabla_h e^k\|_{l^6}^2 \\
&\leq K^4 K_2 \|\nabla_h e^k\|^{\frac{2}{3}} \left(16\|\Delta_h e^k\|^2 + \frac{1}{L^2} \|\nabla_h e^k\|^2 \right)^{\frac{2}{3}} \\
&\leq K^4 K_2 \left[\frac{1}{3} \|\nabla_h e^k\|^2 + \frac{2}{3} \left(16\|\Delta_h e^k\|^2 + \frac{1}{L^2} \|\nabla_h e^k\|^2 \right) \right] \\
&\leq C_4 \sum_{k=1}^n \tau_k (\|\Delta_h e^k\|^2 + \|\nabla_h e^k\|^2), \tag{3.15}
\end{aligned}$$

where $C_4 = \max\{\frac{32}{3}, \frac{1}{3} + \frac{2}{3L^2}\}$. By inserting (3.15) into (3.14), one gets the final estimate

of the third term on the right hand in (3.10)

$$\begin{aligned} & \sum_{k,l}^{n,k} \theta_{k-l}^{(k)} \langle (\nabla_h u^l \cdot \nabla_h e^l) \nabla_h u^l, \nabla_h e^k \rangle \\ & \leq C_4 \varepsilon_1 \sum_{k=1}^n \tau_k (\|\Delta_h e^k\|^2 + \|\nabla_h e^k\|^2) + \frac{m_3}{4m_1 \varepsilon_1} \sum_{k=1}^n \tau_k \|\nabla_h e^k\|^2. \end{aligned} \quad (3.16)$$

Applying Lemma 3.2, it yields the result for the fourth term on the right hand in (3.10)

$$\left| - \sum_{k,l}^{n,k} \theta_{k-l}^{(k)} \langle \nabla_h e^l, \nabla_h e^k \rangle \right| \leq \frac{m_2}{2} \sum_{k=1}^n \tau_k \|\nabla_h e^k\|^2. \quad (3.17)$$

Substituting (3.11), (3.13), (3.16) and (3.17) into (3.10), one has an estimate of the non-linear term

$$\begin{aligned} & \sum_{k,l}^{n,k} \theta_{k-l}^{(k)} \langle f(\nabla_h U^l) - f(\nabla_h u^l), \nabla_h e^k \rangle \\ & \leq C_5 \varepsilon_1 \sum_{k=1}^n \tau_k \|\Delta_h e^k\|^2 + \left(\frac{C_6}{\varepsilon_1} + C_5 \varepsilon_1 + \frac{m_3}{2} \right) \sum_{k=1}^n \tau_k \|\nabla_h e^k\|^2, \end{aligned} \quad (3.18)$$

where $C_5 = 1 + C_3 + C_4$, $C_6 = \frac{m_3}{4m_1} (C_\Omega C_2^2 + 2)$.

Summing up (3.7), (3.8) and (3.18), then it follows from (3.6) that

$$\begin{aligned} & \frac{1}{2} \|e^n\|^2 + \frac{\delta m_1}{2m_2} \sum_{k=1}^n \tau_k \|\Delta_h e^k\|^2 \\ & \leq \frac{1}{2} \|e^0\|^2 + C_5 \varepsilon_1 \sum_{k=1}^n \tau_k \|\Delta_h e^k\|^2 + \left(\frac{C_6}{\varepsilon_1} + C_5 \varepsilon_1 + \frac{m_3}{2} \right) \sum_{k=1}^n \tau_k \|\nabla_h e^k\|^2 \\ & \quad + \sum_{k,l}^{n,k} \theta_{k-l}^{(k)} \langle \xi^l + \eta^l, e^k \rangle \\ & \leq \frac{1}{2} \|e^0\|^2 + C_5 \varepsilon_1 \sum_{k=1}^n \tau_k \|\Delta_h e^k\|^2 + \left(\frac{C_6}{\varepsilon_1} + C_5 \varepsilon_1 + \frac{m_3}{2} \right) \sum_{k=1}^n \tau_k \|\Delta_h e^k\| \|e^k\| \\ & \quad + \sum_{k,l}^{n,k} \theta_{k-l}^{(k)} \langle \xi^l + \eta^l, e^k \rangle \\ & \leq \frac{1}{2} \|e^0\|^2 + \left(C_5 \varepsilon_1 + \left(\frac{C_6}{\varepsilon_1} + C_5 \varepsilon_1 + \frac{m_3}{2} \right) \varepsilon_2 \right) \sum_{k=1}^n \tau_k \|\Delta_h e^k\|^2 + \sum_{k=1}^n \|e^k\| (\|P^k\| + \|Q^k\|) \\ & \quad + \frac{1}{4\varepsilon_2} \left(\frac{C_6}{\varepsilon_1} + C_5 \varepsilon_1 + \frac{m_3}{2} \right) \sum_{k=1}^n \tau_k \|e^k\|^2 \quad \text{for any } \varepsilon_2 > 0, \end{aligned} \quad (3.19)$$

where we have used embedding inequality (2.1) and $P_h^k = \sum_{l=1}^k \theta_{k-l}^{(k)} \xi_h^l$ and $Q_h^k = \sum_{l=1}^k \theta_{k-l}^{(k)} \eta_h^l$. Taking $\varepsilon_1 = \frac{\delta m_1}{4C_5 m_2}$ and $\varepsilon_2 = \delta^2 m_1^2 / (16m_2^2 C_5 C_6 + \delta^2 m_1^2 + 2\delta m_1 m_2 m_3)$, it follows from (3.19)

$$\|e^n\|^2 \leq \|e^0\|^2 + C_7 \sum_{k=1}^n \tau_k \|e^k\|^2 + 2 \sum_{k=1}^n \|e^k\| (\|P^k\| + \|Q^k\|),$$

where $C_7 = \frac{1}{2\varepsilon_2} \left(\frac{C_6}{\varepsilon_1} + C_5 \varepsilon_1 + \frac{m_3}{2} \right)$. Choosing a proper integer n_0 ($0 \leq n_0 \leq n$) such that $\|e^{n_0}\| = \max_{1 \leq k \leq n} \|e^k\|$ and then taking $n = n_0$ in the above inequality, it yields

$$\|e^{n_0}\|^2 \leq \|e^0\| \cdot \|e^{n_0}\| + C_7 \sum_{k=1}^{n_0} \tau_k \|e^k\| \cdot \|e^{n_0}\| + 2 \sum_{k=1}^{n_0} (\|P^k\| + \|Q^k\|) \cdot \|e^{n_0}\|,$$

which leads to

$$\|e^n\| \leq \|e^{n_0}\| \leq \|e^0\| + C_7 \sum_{k=1}^n \tau_k \|e^k\| + 2 \sum_{k=1}^n (\|P^k\| + \|Q^k\|).$$

When $\tau_n \leq \frac{1}{2C_7} := \tau_0$, Lemma 3.7 implies that

$$\|e^n\| \leq 2 \exp(C_7 t_{n-1}) \left(\|e^0\| + 2 \sum_{k=1}^n (\|P^k\| + \|Q^k\|) \right). \quad (3.20)$$

By virtue of Lemma 3.1 and Lemma 3.6, the desired estimate is obtained from (3.20). The proof ends.

4. Numerical experiments

In this section, we provide two numerical examples to verify the convergence rate in time and the energy dissipation. Only simple iteration is used to solve the nonlinear algebra equations at each time level with the tolerance as 10^{-12} and the solution at previous level is chosen as the initial guess. We test the convergence rate on the graded meshes for the first example.

Example 4.1. Consider the MBE model $u_t + \delta \Delta^2 u + f(\nabla_h u) = g(\mathbf{x}, t)$, $\mathbf{x} \in \Omega = (0, 2\pi)^2$, $0 < t \leq 1$ with $\delta = 0.1$. We take the function $g(\mathbf{x}, t)$ such that it has an exact solution $u(\mathbf{x}, t) = \cos t \sin x \sin y$.

The example is to demonstrate the time accuracy of the variable-step BDF2 scheme (2.2) on the graded meshes. Let r be a positive integer, $t_k = T \left(\frac{k}{N} \right)^r$ and $\tau_k = t_k - t_{k-1}$. Denote the discrete L^2 norm error $e(N) := \|U^N - u^N\|$ and the order of convergence in time direction is defined by $\text{Order} = \log_2(e(N)/e(2N))$. The number of the spatial grid

Table 1: Errors and convergence rate of the variable-step BDF2 scheme (2.2)

N	$e(N)$	Order
40	1.03e-04	–
80	2.82e-05	1.87
160	6.74e-06	2.06
320	1.60e-06	2.07

points are fixed as $M = 3000$. We list the numerical results, including the L^2 norm error $e(N)$, the order of convergence in time direction. From Table 1, it is easily verified that the variable-step BDF2 scheme (2.2) achieves second-order accuracy in time as proved in Theorem 3.1.

Next, adaptive time-stepping strategy, which is designed to capture the multi-scale behavior of the gradient flow, is utilized to compute the MBE model (1.1) in the implementation of the variable-step BDF2 scheme. We adopt the commonly used time adaptive strategy of [[48] Algorithm 1] to get the variation of the time steps. In detail, the time-step τ_{ada} is updated adaptively using the current step information τ_{cur} by the formula $\tau_{ada}(e, \tau_{cur}) = \min\{\sqrt{tol/e\rho}\tau_{cur}\}$, where ρ is a default safety coefficient, tol is a reference tolerance and e is the relative error at each time level. Moreover, τ_{max} and τ_{min} are predetermined maximum and minimum time steps respectively. In the following simulation, we choose the safety coefficient as $\rho = 0.9$, the reference tolerance $tol = 10^{-3}$, the maximum time step $\tau_{max} = 0.1$ and the minimum time step $\tau_{min} = 10^{-4}$.

Algorithm 4.1 Adaptive time-stepping strategy

Require: Set $\tau_1 := \tau_{min}$. Given u^n and time step τ_n

- 1: Compute u^{n+1} by using BDF2 scheme with time step τ_n .
 - 2: Calculate $e_{n+1} = \|u^{n+1} - u^n\|/\|u^{n+1}\|$.
 - 3: **if** $e_n < tol$ or $\tau_n \leq \tau_{min}$ **then**
 - 4: **if** $e_n < tol$ **then**
 - 5: Update time-step size $\tau_{n+1} \leftarrow \min\{\max\{\tau_{min}, \tau_{ada}\}, 2.414\tau_n, \tau_{max}\}$.
 - 6: **else**
 - 7: Update time-step size $\tau_{n+1} \leftarrow \tau_{min}$.
 - 8: **end if**
 - 9: **else**
 - 10: Recalculate with time-step size $\tau_n \leftarrow \max\{\tau_{min}, \tau_{ada}\}$.
 - 11: Goto 1
 - 12: **end if**
-

In addition, we use the roughness measure function $R(t)$ as defined in [36]:

$$R(t) = \sqrt{\frac{1}{|\Omega|} \int_{\Omega} (u(x, y, t) - \bar{u}(x, y, t))^2 dx},$$

where $\bar{u}(x, y, t) = \frac{1}{|\Omega|} \int_{\Omega} u(x, y, t) dx$. It will be tested also in the next example.

Example 4.2. Take $\Omega = (0, 2\pi)^2$. Consider the problem (1.1) with the initial condition as follows

$$u(x, y, 0) = 0.1(\sin 3x \sin 2y + \sin 5x \sin 5y).$$

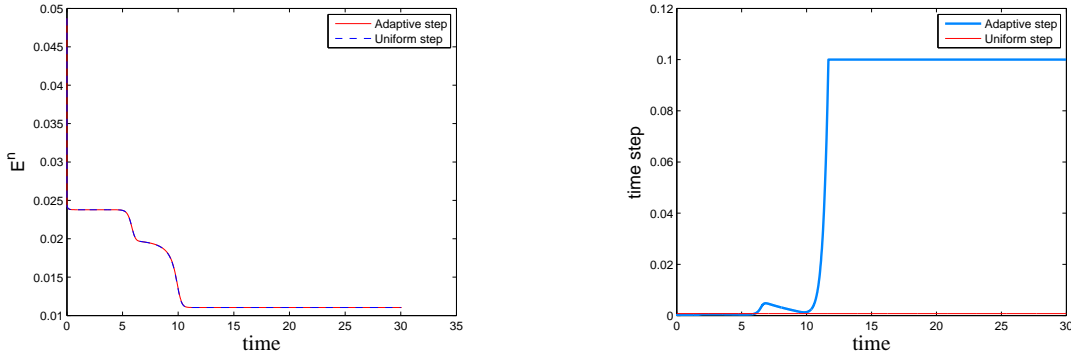


Figure 1: Comparisons of the energy (left) and the time steps (right) of the BDF2 scheme (2.2) using the fixed time steps and the adaptive time strategies.

We take the parameter $\delta = 0.1$ and a 128×128 uniform mesh to discrete the spatial domain $\Omega = (0, 2\pi)^2$. In order to make the comparisons, we simulate the MBE model until $T = 30$ on the uniform time meshes with the fixed time step $\tau = 10^{-3}$ and the adaptive time meshes (described in Algorithm 1), respectively. In Figure 1, the time evolutions of discrete energies (left) and the corresponding time-step sizes (right) are depicted. From Figure 1, we observe that the discrete energy curve on the adaptive time steps is in accordance with that generated by using a small constant step size. In addition, Figure 1 also demonstrates that the adaptive BDF2 scheme (2.2) is more efficient computationally that small time steps are chosen when the energy decays fast while large time steps are automatically selected when the energy dissipates slowly.

In Figure 2, we plot the time evolution of the roughness measure function $R(t)$. The time evolution curve of $R(t)$ displays that the deviation decreases for a short period and then keeps increasing until the steady-state. In Figure 3, the snapshots of the numerical solutions u are shown until the steady-state by the adaptive BDF2 scheme (2.2).

Acknowledgement

We would like to acknowledge support by the National Natural Science Foundation of China (No. 11701229, 11701081, 11861060), the Jiangsu Provincial Key Laboratory of Networked

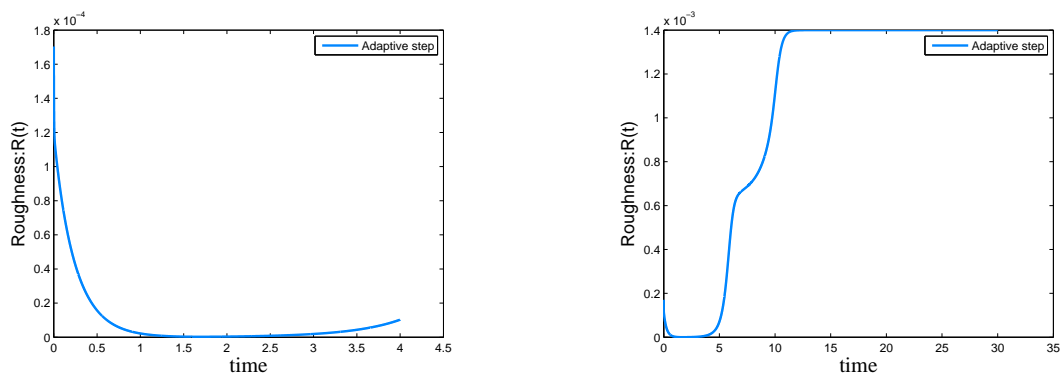


Figure 2: Roughness evolution for MBE as $t = 4$ (left) and $t = 30$ (right) .

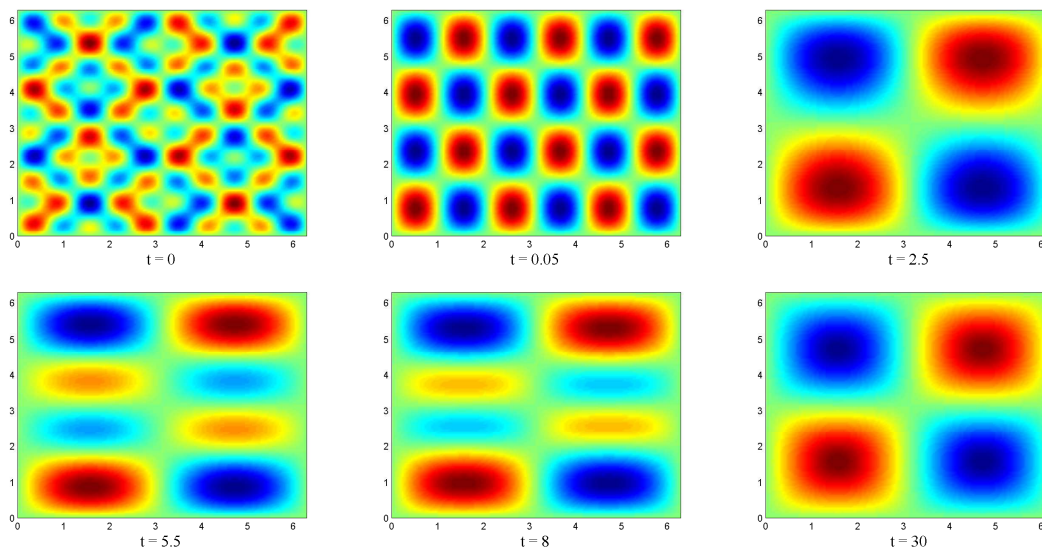


Figure 3: Evolution of the solutions by the BDF2 scheme (2.2) using the adaptive time strategy at $t = 0, 0.05, 2.5, 5.5, 8, 30$.

Collective Intelligence (No. BM2017002), Key Project of Natural Science Foundation of China (No. 61833005) and ZhiShan Youth Scholar Program of SEU, China Postdoctoral Science Foundation (No. 2019M651634), High-level Scientific Research foundation for the introduction of talent of Nanjing Institute of Technology (No. YKL201856).

Appendix

We give the detailed proofs of Lemma 3.2 - Lemma 3.5 in the Appendix. Two fundamental properties of the time discretization coefficients are provided in order to show the proofs. We start with the introduction of the following two matrices

$$\mathbf{B}_2 = \begin{pmatrix} b_0^{(1)} & & & & \\ b_1^{(2)} & b_0^{(2)} & & & \\ & \ddots & \ddots & & \\ & & & b_1^{(n)} & b_0^{(n)} \end{pmatrix} \otimes \mathbf{I}_2, \quad \Theta_2 = \begin{pmatrix} \theta_0^{(1)} & & & & \\ \theta_1^{(2)} & \theta_0^{(2)} & & & \\ \vdots & \ddots & \ddots & & \\ \theta_{n-1}^{(n)} & \dots & \theta_1^{(n)} & \theta_0^{(n)} \end{pmatrix} \otimes \mathbf{I}_2,$$

where the elements $b_{n-k}^{(n)}$ and $\theta_{n-k}^{(n)}$ are defined by (2.3) and (2.4), respectively, \mathbf{I}_2 is 2×2 identity matrix and \otimes is tensor product. By virtue of the discrete orthogonal identity (2.5), it yields $\Theta_2 = \mathbf{B}_2^{-1}$. Denote $\mathbf{B} = \mathbf{B}_2 + \mathbf{B}_2^T$ and $\Theta = \Theta_2 + \Theta_2^T$, then it follows from Lemma 2.2 and Lemma 3.1 that the matrix \mathbf{B} and Θ are symmetric and positive definite. By substitution of Θ with \mathbf{B}_2 , we have

$$\Theta := \mathbf{B}_2^{-1} + (\mathbf{B}_2^{-1})^T = (\mathbf{B}_2^{-1})^T \mathbf{B} \mathbf{B}_2^{-1}. \quad (\text{A.1})$$

In addition, we define a diagonal matrix $\Lambda_\tau = \text{diag}(\sqrt{\tau_1}, \sqrt{\tau_2}, \dots, \sqrt{\tau_n}) \otimes \mathbf{I}_2$ and denote

$$\tilde{\mathbf{B}}_2 := \Lambda_\tau \mathbf{B}_2 \Lambda_\tau = \tilde{\mathbf{B}}_2 \otimes \mathbf{I}_2 \quad \text{and} \quad \tilde{\Theta}_2 := \tilde{\mathbf{B}}_2^{-1} \otimes \mathbf{I}_2,$$

$$\text{where } \tilde{\mathbf{B}}_2 = \begin{pmatrix} \tilde{b}_0^{(1)} & & & & \\ \tilde{b}_1^{(2)} & \tilde{b}_0^{(2)} & & & \\ & \ddots & \ddots & & \\ & & & \tilde{b}_1^{(n)} & \tilde{b}_0^{(n)} \end{pmatrix} \quad \text{and} \quad \tilde{\Theta}_2 := \tilde{\mathbf{B}}_2^{-1} = \begin{pmatrix} \tilde{\theta}_0^{(1)} & & & & \\ \tilde{\theta}_1^{(2)} & \tilde{\theta}_0^{(2)} & & & \\ \vdots & \vdots & \ddots & & \\ \tilde{\theta}_{n-1}^{(n)} & \tilde{\theta}_{n-2}^{(n)} & \dots & \tilde{\theta}_0^{(n)} \end{pmatrix}.$$

It is easy to check that $\tilde{b}_0^{(1)} = 2$, $\tilde{b}_0^{(k)} = \frac{1+2r_k}{1+r_k}$ and $\tilde{b}_1^{(k)} = -\frac{r_k^{\frac{3}{2}}}{1+r_k}$, $2 \leq k \leq n$. It follows from Lemma 3.1 that

$$\tilde{\theta}_{k-j}^{(k)} = \frac{1}{\sqrt{\tau_k \tau_j}} \theta_{k-j}^{(k)} = \frac{1+r_j}{1+2r_j} \prod_{i=j+1}^k \frac{r_i^{\frac{3}{2}}}{1+2r_i}, \quad 1 \leq j \leq k \leq n. \quad (\text{A.2})$$

Define the symmetric matrix $\tilde{\mathbf{B}} := \tilde{\mathbf{B}}_2 + \tilde{\mathbf{B}}_2^T = \Lambda_\tau \mathbf{B} \Lambda_\tau$. We introduce the vector norm $\|\cdot\|$ by $\|\mathbf{u}\| = \sqrt{\mathbf{u}^T \mathbf{u}}$ and the associated matrix norm $\|\mathbf{A}\| := \sqrt{\rho(\mathbf{A}^T \mathbf{A})}$.

The proof of Lemma 3.2 Firstly, we estimate the lower bound of $\lambda_{\min}(\tilde{\mathbf{B}})$ and the upper bound of $\lambda_{\max}(\tilde{\mathbf{B}}_2^T \tilde{\mathbf{B}}_2)$. Denote λ be the eigenvalue of the matrix $\tilde{\mathbf{B}}$. By use of the

Gerschgorin's circle theorem, one arrives at $|\lambda - 2\tilde{b}_0^{(k)}| \leq |\tilde{b}_1^{(k)}| + |\tilde{b}_1^{(k+1)}|$, $2 \leq k \leq n-1$. Then it yields

$$\lambda_{\min}(\tilde{\mathbf{B}}) \geq \min_{1 \leq k \leq n} \left\{ \frac{2 + 4r_k - r_k^{\frac{3}{2}}}{1 + r_k} - \frac{r_{k+1}^{\frac{3}{2}}}{1 + r_{k+1}} \right\} \geq \frac{2 + 2r_s(2 - \sqrt{r_s})}{1 + r_s} := m_1. \quad (\text{A.3})$$

By applying the properties of the Kronecker tensor product $(A \otimes B)^T = A^T \otimes B^T$ and $(A \otimes B)(C \otimes D) = AC \otimes BD$, we have $\tilde{\mathbf{B}}_2^T \tilde{\mathbf{B}}_2 = (\tilde{\mathbf{B}}_2^T \tilde{\mathbf{B}}_2) \otimes \mathbf{I}_2$. Making use of the Gerschgorin's circle theorem, it leads to

$$\lambda_{\max}(\tilde{\mathbf{B}}_2^T \tilde{\mathbf{B}}_2) \leq \max_{2 \leq k \leq n} \{\mathfrak{R}(r_k, r_{k+1}), 3 + \mathfrak{R}(r_1, r_2)\} \leq 3 + \mathfrak{R}(r_s, r_s) := m_2,$$

where $r_1 = 0$ and the function $\mathfrak{R}(u, v)$ is defined by

$$\mathfrak{R}(u, v) = \frac{(1 + 2u)(1 + 2u + u^{\frac{3}{2}})}{(1 + u)^2} + \frac{v^{\frac{3}{2}}(1 + 2v + v^{\frac{3}{2}})}{(1 + v)^2}, \quad 0 \leq u, v \leq r_s.$$

Then we obtain

$$\lambda_{\max}(\tilde{\mathbf{B}}_2^T \tilde{\mathbf{B}}_2) \leq m_2. \quad (\text{A.4})$$

Denote $\mathbf{v} = ((\mathbf{v}^1)^T, (\mathbf{v}^2)^T, \dots, (\mathbf{v}^n)^T)^T$. The inequality (A.3) implies that the symmetric matrix $\tilde{\mathbf{B}}$ is positive definite. There exists a non-singular upper triangular matrix $\tilde{\mathbf{U}}$ such that $\tilde{\mathbf{B}} = \tilde{\mathbf{U}}^T \tilde{\mathbf{U}}$. Then we obtain

$$\mathbf{v}^T \Theta \mathbf{v} = \mathbf{v}^T (\mathbf{B}_2^{-1})^T \mathbf{B} \mathbf{B}_2^{-1} \mathbf{v} = \mathbf{v}^T (\mathbf{B}_2^{-1})^T \Lambda_\tau^{-1} \tilde{\mathbf{B}} \Lambda_\tau^{-1} \mathbf{B}_2^{-1} \mathbf{v} = \|\tilde{\mathbf{U}} \Lambda_\tau^{-1} \mathbf{B}_2^{-1} \mathbf{v}\|^2.$$

Consequently, it yields

$$\begin{aligned} \|\Lambda_\tau \mathbf{v}\|^2 &= \|\Lambda_\tau \mathbf{B}_2 \Lambda_\tau \tilde{\mathbf{U}}^{-1} \tilde{\mathbf{U}} \Lambda_\tau^{-1} \mathbf{B}_2^{-1} \mathbf{v}\|^2 \\ &\leq \|\tilde{\mathbf{B}}_2 \tilde{\mathbf{U}}^{-1}\|^2 \|\tilde{\mathbf{U}} \Lambda_\tau^{-1} \mathbf{B}_2^{-1} \mathbf{v}\|^2 \\ &\leq \|\tilde{\mathbf{B}}_2\|^2 \|\tilde{\mathbf{U}}^{-1}\|^2 \mathbf{v}^T \Theta \mathbf{v} \\ &= \lambda_{\max}(\tilde{\mathbf{B}}_2^T \tilde{\mathbf{B}}_2) \lambda_{\max}(\tilde{\mathbf{B}}^{-1}) \mathbf{v}^T \Theta \mathbf{v}. \end{aligned}$$

It follows from (A.3) and (A.4) that

$$\mathbf{v}^T \Theta \mathbf{v} \geq \frac{m_1}{m_2}. \quad (\text{A.5})$$

Let $\tilde{\Theta} = \tilde{\Theta}_2 + \tilde{\Theta}_2^T$. Noticing $0 < \frac{x^{3/2}}{1+2x} < m_* : \frac{r_s^{3/2}}{1+2r_s} < 1$ for any $x \in [0, r_s)$, we have

$$\mathfrak{R}_{n,k} := \sum_{j=1}^k \tilde{\theta}_{k-j}^{(k)} + \sum_{j=k}^n \theta_{j-k}^{(j)} \leq \sum_{j=1}^k m_*^{k-j} + \sum_{j=k}^n m_*^{j-k} < \frac{2}{1-m_*}, \quad 1 \leq k \leq n.$$

Using Gerschgorin's circle theorem, one arrives at $\lambda_{\max}(\tilde{\Theta}) \leq \max_{1 \leq k \leq n} \mathfrak{R}_{n,k} < m_3 := \frac{2}{1-m_*}$. Thus it leads to $\mathbf{w}^T \tilde{\Theta} \mathbf{w} \leq m_3 \|\mathbf{w}\|^2$ for any \mathbf{w} , where $\tilde{\Theta} := \tilde{\Theta} \otimes I_2$. By taking $\mathbf{w} := \Lambda_\tau \mathbf{v}$, it yields

$$\mathbf{v}^T \Theta \mathbf{v} \leq m_3 \|\Lambda_\tau \mathbf{v}\|^2. \quad (\text{A.6})$$

Combining (A.5) and (A.6) and using the fact $\mathbf{v}^T \Theta \mathbf{v} = 2 \sum_{k,l}^{n,k} \theta_{k-l}^{(k)} (\mathbf{v}^k)^T \mathbf{v}^l$, it yields the desired result.

The proof of Lemma 3.3 Let $\mathbf{w} = ((\mathbf{w}^1)^T, (\mathbf{w}^2)^T, \dots, (\mathbf{w}^n)^T)^T$. A similar proof of Lemma A.3 in [46] yields

$$\sum_{k,j}^{n,k} \theta_{k-j}^{(k)} (\mathbf{v}^j)^T \mathbf{w}^k \leq \varepsilon \sum_{k,j}^{n,k} \theta_{k-j}^{(k)} (\mathbf{v}^j)^T \mathbf{v}^k + \frac{1}{2\varepsilon} \mathbf{w}^T \mathbf{B}^{-1} \mathbf{w} \text{ for any } \varepsilon > 0.$$

It is easy to obtain $\mathbf{B}^{-1} = \Lambda_\tau \tilde{\mathbf{U}}^{-1} (\Lambda_\tau \tilde{\mathbf{U}}^{-1})^T$. It follows that

$$\begin{aligned} \mathbf{w}^T \mathbf{B}^{-1} \mathbf{w} &= \|(\tilde{\mathbf{U}}^{-1})^T \Lambda_\tau \mathbf{w}\|^2 \leq \|(\tilde{\mathbf{U}}^{-1})^T\|^2 \|\Lambda_\tau \mathbf{w}\|^2 \\ &= \lambda_{\max}(\tilde{\mathbf{B}}^{-1}) \mathbf{w}^T \Lambda_\tau^2 \mathbf{w} \leq m_1^{-1} \sum_{k=1}^n \tau_k (\mathbf{w}^k)^2. \end{aligned}$$

Consequently, we have

$$\sum_{k,j}^{n,k} \theta_{k-j}^{(k)} (\mathbf{v}^j)^T \mathbf{w}^k \leq \varepsilon \sum_{k,j}^{n,k} \theta_{k-j}^{(k)} (\mathbf{v}^j)^T \mathbf{v}^k + \frac{1}{2m_1 \varepsilon} \sum_{k=1}^n \tau_k (\mathbf{w}^k)^2 \text{ for any } \varepsilon > 0.$$

By choosing $\varepsilon = 2\varepsilon/m_3$ in the above inequality and using (A.6), one gets

$$\sum_{k,j}^{n,k} \theta_{k-j}^{(k)} (\mathbf{v}^j)^T \mathbf{w}^k \leq \varepsilon \sum_{k=1}^n \tau_k (\mathbf{v}^k)^T \mathbf{v}^k + \frac{m_3}{4m_1 \varepsilon} \sum_{k=1}^n \tau_k (\mathbf{w}^k)^T \mathbf{w}^k.$$

The proof of Lemma 3.4 For the fixed time index n , by taking $\mathbf{v}^j := u^j \mathbf{z}^j$ and $\varepsilon := \varepsilon_1$ in Lemma 3.3, it yields

$$\sum_{k,j}^{n,k} \theta_{k-j}^{(k)} \langle u^j \mathbf{z}^j, \mathbf{w}^k \rangle \leq \varepsilon_1 \sum_{k=1}^n \tau_k \|u^k \mathbf{z}^k\|^2 + \frac{m_3}{4m_1 \varepsilon_1} \sum_{k=1}^n \tau_k \|\mathbf{w}^k\|^2.$$

With the help of Hölder inequality, one has $\|u^k \mathbf{z}^k\| \leq \|u^k\|_{l^3} \|\mathbf{z}^k\|_{l^6}$. The embedding inequal-

ity $\|\mathbf{z}^k\|_{l_6}^2 \leq C_\Omega(\|\nabla_h \mathbf{z}^k\|^2 + \|\mathbf{z}^k\|^2)$ yields

$$\begin{aligned} \sum_{k=1}^n \tau_k \|u^k \mathbf{z}^k\|^2 &\leq \sum_{k=1}^n \tau_k \|u^k\|_{l_3}^2 \|\mathbf{z}^k\|_{l_6}^2 \\ &\leq C_\Omega \sum_{k=1}^n \tau_k \|u^k\|_{l_3}^2 (\|\nabla_h \mathbf{z}^k\|^2 + \|\mathbf{z}^k\|^2) \\ &\leq C_u^2 C_\Omega \sum_{k=1}^n \tau_k (\|\nabla_h \mathbf{z}^k\|^2 + \|\mathbf{z}^k\|^2). \end{aligned}$$

It follows from the above inequality that

$$\sum_{k,j}^{n,k} \theta_{k-j}^{(k)} \langle u^j \mathbf{z}^j, \mathbf{w}^k \rangle \leq \varepsilon_1 C_u^2 C_\Omega \sum_{k=1}^n \tau_k (\|\nabla_h \mathbf{z}^k\|^2 + \|\mathbf{z}^k\|^2) + \frac{m_3}{4m_1 \varepsilon_1} \sum_{k=1}^n \tau_k \|\mathbf{w}^k\|^2. \quad (\text{A.7})$$

Taking $\varepsilon = \varepsilon_1 C_u^2 C_\Omega$, one gets the claimed inequality.

The proof of Lemma 3.5 For any integers $1 \leq s \leq m \leq M$, we have

$$\begin{aligned} |\Delta_x u_{mj}|^3 - |\Delta_x u_{sj}|^3 &= \sum_{i=s}^{m-1} (|\Delta_x u_{i+1,j}|^3 - |\Delta_x u_{ij}|^3) \\ &= \sum_{i=s}^{m-1} (|\Delta_x u_{i+1,j}| - |\Delta_x u_{ij}|) (|\Delta_x u_{i+1,j}|^2 + |\Delta_x u_{ij}| \cdot |\Delta_x u_{i+1,j}| + |\Delta_x u_{ij}|^2) \\ &\leq 2h \sum_{i=s}^{m-1} \left| \frac{\Delta_x u_{i+1,j} - \Delta_x u_{ij}}{h} \right| \cdot (|\Delta_x u_{i+1,j}|^2 + |\Delta_x u_{ij}|^2) \\ &= h \sum_{i=s}^{m-1} |\delta_x^2 u_{i+1,j} + \delta_x^2 u_{ij}| \cdot (|\Delta_x u_{i+1,j}|^2 + |\Delta_x u_{ij}|^2) \\ &\leq 4 \left(h \sum_{i=1}^M |\delta_x^2 u_{ij}|^2 \right)^{\frac{1}{2}} \left(h \sum_{i=1}^M |\Delta_x u_{ij}|^4 \right)^{\frac{1}{2}}. \end{aligned}$$

It is easy to verify the above inequality also holds for $m \leq s$. Then, it follows that

$$|\Delta_x u_{mj}|^3 \leq 4 \left(h \sum_{i=1}^M |\delta_x^2 u_{ij}|^2 \right)^{\frac{1}{2}} \left(h \sum_{i=1}^M |\Delta_x u_{ij}|^4 \right)^{\frac{1}{2}} + |\Delta_x u_{sj}|^3, \quad 1 \leq m, s \leq M.$$

Multiplying the above inequality by h and summing up s from 1 to M , it yields

$$L |\Delta_x u_{mj}|^3 \leq 4L \left(h \sum_{i=1}^M |\delta_x^2 u_{ij}|^2 \right)^{\frac{1}{2}} \left(h \sum_{i=1}^M |\Delta_x u_{ij}|^4 \right)^{\frac{1}{2}} + h \sum_{i=1}^M |\Delta_x u_{ij}|^3.$$

The above inequality holds for $m = 1, 2, \dots, M$, one can get

$$\max_{1 \leq m \leq M} |\Delta_x u_{mj}|^3 \leq 4 \left(h \sum_{i=1}^M |\delta_x^2 u_{ij}|^2 \right)^{\frac{1}{2}} \left(h \sum_{i=1}^M |\Delta_x u_{ij}|^4 \right)^{\frac{1}{2}} + \frac{1}{L} h \sum_{i=1}^M |\Delta_x u_{ij}|^3.$$

Multiplying the above inequality by h , and summing up j from 1 to M , we have

$$\begin{aligned} h \sum_{j=1}^M \max_{1 \leq m \leq M} |\Delta_x u_{mj}|^3 &\leq 4h \sum_{j=1}^M \left(h \sum_{i=1}^M |\delta_x^2 u_{ij}|^2 \right)^{\frac{1}{2}} \left(h \sum_{i=1}^M |\Delta_x u_{ij}|^4 \right)^{\frac{1}{2}} + \frac{1}{L} \|\Delta_x u\|_3^3 \\ &\leq 4 \left(h^2 \sum_{i=1}^M \sum_{j=1}^M |\delta_x^2 u_{ij}|^2 \right)^{\frac{1}{2}} \left(h^2 \sum_{i=1}^M \sum_{j=1}^M |\Delta_x u_{ij}|^4 \right)^{\frac{1}{2}} + \frac{1}{L} \|\Delta_x u\|_3^3. \end{aligned} \quad (\text{A.8})$$

By Cauchy-Schwarz inequality, we obtain

$$\|\Delta_x u\|_3^3 \leq \left(h^2 \sum_{i=1}^M \sum_{j=1}^M |\Delta_x u_{ij}|^2 \right)^{\frac{1}{2}} \cdot \left(h^2 \sum_{i=1}^M \sum_{j=1}^M |\Delta_x u_{ij}|^4 \right)^{\frac{1}{2}} = \|\Delta_x u\| \cdot \|\Delta_x u\|_4^2.$$

Substituting the above inequality into (A.8), we have

$$h \sum_{j=1}^M \max_{1 \leq m \leq M} |\Delta_x u_{mj}|^3 \leq \|\Delta_x u\|_4^2 \left(4 \|\delta_x^2 u\| + \frac{1}{L} \|\Delta_x u\| \right). \quad (\text{A.9})$$

Besides, it is also valid

$$|\Delta_x u_{im}|^3 - |\Delta_x u_{is}|^3 = \sum_{j=s}^{m-1} \left(|\Delta_x u_{i,j+1}|^3 - |\Delta_x u_{ij}|^3 \right).$$

Similar to the previous process, it yields

$$h \sum_{j=1}^M \max_{1 \leq m \leq M} |\Delta_x u_{mj}|^3 \leq \|\Delta_x u\|_4^2 \left(4 \|\delta_x \delta_y u\| + \frac{1}{L} \|\Delta_x u\| \right). \quad (\text{A.10})$$

We now estimate $\|\Delta_x u\|_6$. Using Cauchy-Schwarz inequality, we have

$$\begin{aligned} h^2 \sum_{i=1}^M \sum_{j=1}^M |\Delta_x u_{ij}|^6 &= h \sum_{i=1}^M \left(h \sum_{j=1}^M |\Delta_x u_{ij}|^3 \cdot |\Delta_x u_{ij}|^3 \right) \\ &\leq h \sum_{i=1}^M \left(\max_{1 \leq j \leq M} |\Delta_x u_{ij}|^3 \cdot h \sum_{j=1}^M |\Delta_x u_{ij}|^3 \right) \\ &\leq \left(h \sum_{i=1}^M \max_{1 \leq j \leq M} |\Delta_x u_{ij}|^3 \right) \left(h \sum_{j=1}^M \max_{1 \leq i \leq M} |\Delta_x u_{ij}|^3 \right) \end{aligned}$$

Substituting (A.9) and (A.10) into above inequality, it leads to

$$\begin{aligned} \|\Delta_x u\|_6^6 &\leq \|\Delta_x u\|_4^4 \left(4 \|\delta_x^2 u\| + \frac{1}{L} \|\Delta_x u\| \right) \left(4 \|\delta_x \delta_y u\| + \frac{1}{L} \|\Delta_x u\| \right) \\ &\leq 5 \|\nabla_h u\|_4^4 \left(4 \|\Delta_h u\|^2 + \frac{1}{L^2} \|\nabla_h u\|^2 \right). \end{aligned}$$

Similarly, we obtain

$$\|\Delta_y u\|_6^6 \leq 5\|\nabla_h u\|_4^4 \left(4\|\Delta_h u\|^2 + \frac{1}{L^2}\|\nabla_h u\|^2\right).$$

Then it follows that

$$\begin{aligned} \|\nabla_h u\|_6^6 &= h^2 \sum_{i=1}^M \sum_{j=1}^M \left(|\Delta_x u_{ij}|^2 + |\Delta_y u_{ij}|^2\right)^3 \\ &\leq 4h^2 \sum_{i=1}^M \sum_{j=1}^M \left(|\Delta_x u_{ij}|^6 + |\Delta_y u_{ij}|^6\right) \\ &\leq 40\|\nabla_h u\|_4^4 \left(4\|\Delta_h u\|^2 + \frac{1}{L^2}\|\nabla_h u\|^2\right). \end{aligned}$$

Following the same procedure of the proof for $\|\nabla_h u\|_6$, we obtain the estimate of $\|\nabla_h u\|_4$

$$\|\nabla_h u\|_4 \leq C_2 \|\nabla_h u\|^{\frac{1}{2}} \left(2\|\Delta_h u\|^2 + \frac{1}{L^2}\|\nabla_h u\|^2\right)^{\frac{1}{4}},$$

where C_2 is a constant. The above two inequalities imply that there exists a constant K such that

$$\|\nabla_h u\|_6 \leq K \|\nabla_h u\|^{\frac{1}{3}} \left(4\|\Delta_h u\|^2 + \frac{1}{L^2}\|\nabla_h u\|^2\right)^{\frac{1}{3}}.$$

References

- [1] M. Y. Li, Y. M. Shi, C. C. Cheng et al., *Epitaxial growth of a monolayer WSe₂-MoS₂ lateral p-n junction with an atomically sharp interface*, Science, **349**, 524–528 (2015).
- [2] L. Wang, X. Z. Xu, L. N. Zhang et al., *Epitaxial growth of a 100-square-centimetre single-crystal hexagonal boron nitride monolayer on copper*, Nature, **570**, 91–95 (2019).
- [3] B. Jenichen, M. Hanke, S. Gaucher et al., *Ordered structure of FeGe₂ formed during solid-phase epitaxy*, Phys. Rev. Mater., **2**, 051402 (2018).
- [4] H. P. Nair, J. P. Ruf, N. J. Schreiber et al., *Demystifying the growth of superconducting Sr₂RuO₄ thin films*, APL Mater., **6**, 101108 (2018).
- [5] D. Moldovan and L. Golubovic, *Interfacial coarsening dynamics in epitaxial growth with slope selection*, Phys. Rev. E (3), **61**, 6190–6214 (2000).
- [6] M. F. Gyure, J. J. Zinck, C. Ratsch, D. D. Vvedensky, *Unstable growth on rough surface*, Phys. Rev. Lett., **81**, 4931–4934 (2003).
- [7] B. B. King, O. Stein and M. Winkler, *A fourth order parabolic equation modelling epitaxial thin film growth*, Preprint No. 94, Department of Mathematics-C, Aachen University, (2000).
- [8] B. Li and J. G. Liu, *Thin film epitaxy with or without slope selection*, European J. Appl. Math., **14**, 713–743 (2003).
- [9] D. Li, Z. H. Qiao and T. Tang, *Gradient bounds for a thin film epitaxy equation*, J. Differ. Equ., **262**, 1720–1746 (2017).

- [10] Z. H. Qiao, Z. Z. Sun and Z. R. Zhang, *The stability and convergence of two linearized finite difference schemes for the nonlinear epitaxial growth model*, Numer. Methods Partial Differential Eq., **28**, 1893–1915 (2012).
- [11] X. F. Yang, J. Zhao and Q. Wang, *Numerical approximations for the molecular beam epitaxial growth model based on the invariant energy quadratization method*, J. Comput. Phys., **333**, 104–127 (2017).
- [12] L. Z. Chen, J. Zhao and X. F. Yang, *Regularized linear schemes for the molecular beam epitaxy model with slope selection*, Appl. Numer. Math., **128**, 139–156 (2018).
- [13] L. Z. Chen, J. Zhao and Y. Z. Gong, *A novel second-order scheme for the molecular beam epitaxy model with slope selection*, Commun. Comput. Phys., **25**, 1024–1044 (2019).
- [14] W. J. Li, W. B. Chen, C. Wang, Y. Yan and R. J. He, *A second order energy stable linear scheme for a thin film model without slope selection*, J. Sci. Comput., **76**, 1905–1937 (2018).
- [15] K. L. Cheng, Z. H. Qiao and C. Wang, *A third order exponential time differencing numerical scheme for no-slope-selection epitaxial thin film model with energy stability*, J. Sci. Comput., **81**, 154–185 (2019).
- [16] W. B. Chen, W. J. Li, C. Wang et al., *Energy stable higher-order linear ETD multi-step methods for gradient flows: application to thin film epitaxy*, Res. Math. Sci., **7**, 13 (2020).
- [17] W. B. Chen, W. J. Li, Z. W. Luo, C. Wang and X. M. Wang, *A stabilized second order exponential time differencing multistep method for thin film growth model without slope selection*, ESAIM-Math. Model. Numer. Anal., **54**, 727–750 (2020).
- [18] H. Zhang, X. F. Yang and J. Zhang, *Stabilized invariant energy quadratization(S-IEQ) method for the molecular beam epitaxial model without slope selection*, Int. J. Numer. Anal. Model., **18**, 642–655 (2021).
- [19] D. Li, C. Y. Qian and W. Yang, *Correction to: The BDF3/EP3 scheme for MBE with no slope selection is stable*, J. Sci. Comput., **89**, 62 (2021).
- [20] Y. H. Hao, Q. M. Huang and C. Wang, *A third order BDF energy stable linear scheme for the no-slope-selection thin film model*, Commun. Comput. Phys., **29**, 905–929 (2021).
- [21] C. J. Xu and T. Tang, *Stability analysis of large time-stepping methods for epitaxial growth models*, SIAM J. Numer. Anal., **44**, 1759–1779 (2006).
- [22] D. Li, Z. Qiao and T. Tang, *Characterizing the stabilization size for semi-implicit Fourier-spectral method to phase field equations*, SIAM J. Numer. Anal., **54**, 1653–1681 (2016).
- [23] W. Q. Feng, C. Wang, S. M. Wise and Z. R. Zhang, *A second-order energy stable backward differentiation formula method for the epitaxial thin film equation with slope selection*, Numer. Meth. Part Differ. Equ., **34**, 1975–2007 (2018).
- [24] S. F. Wang, W. B. Chen, H. S. Pan and C. Wang, *Optimal rate convergence analysis of a second order scheme for a thin film model with slope selection*, J. Comput. Appl. Math., **377**, 112855 (2020).
- [25] W. B. Chen, C. Wang, X. M. Wang and S. M. Wise, *A linear iteration algorithm for a second-order energy stable scheme for a thin film model without slope selection*, J. Sci. Comput., **57**, 574–601 (2014).
- [26] W. B. Chen, Y. C. Zhang, W. J. Li, Y. Q. Wang and Y. Yan, *Optimal convergence analysis of a second order scheme for a thin film model without slope selection*, J. Sci. Comput., **80**, 1716–1730 (2019).
- [27] W. B. Chen and Y. Q. Wang, *A mixed finite element method for thin film epitaxy*, Numer. Math., **122**, 771–793 (2012).
- [28] Z. H. Qiao, T. Tang, H. H. Xie, *Error analysis of a mixed finite element method for the molecular beam epitaxy model*, SIAM J. Numer. Anal. **53**, 184–205 (2015).
- [29] F. S. Luo, H. H. Xie, M. T. Xie et al., *Adaptive time-stepping algorithms for molecular beam*

- epitaxy: *Based on energy or roughness*, Appl. Math. Lett., **99**, 105991 (2020).
- [30] Z. H. Qiao, Z. Z. Sun, and Z. R. Zhang, *Stability and convergence of second-order schemes for the nonlinear epitaxial growth model without slope selection*, Math. Comput., **84**, 653–674 (2015).
- [31] Y. Y. Kang and H. L. Liao, *Energy stability of BDF methods up to fifth-order for the molecular beam epitaxial model without slope selection*, J. Sci. Comput., **91**, 47 (2022).
- [32] Y. Z. Cheng, A. Kurganov, Z. L. Qu and T. Tang, *Fast and stable explicit operator splitting methods for phase-field models*, J. Comput. Phys., **303**, 45–65 (2015).
- [33] X. Li, Z. H. Qiao, H. Zhang, *Convergence of a fast explicit operator splitting method for the epitaxial growth model with slope selection*, SIAM J. Numer. Anal., **55**, 265–285 (2017).
- [34] H. G. Lee, J. Shin and J. Y. Lee, *A second-order operator splitting Fourier spectral method for models of epitaxial thin film growth*, J. Sci. Comput., **71**, 1303–1318 (2017).
- [35] X. L. Feng, T. Tang and J. Yang, *Long time numerical simulations for phase-field problems using p -adaptive spectral deferred correction methods*, SIAM J. Sci. Comput., **37**, A271–A294 (2015).
- [36] C. Wang, X. M. Wang and S. M. Wise, *Unconditionally stable schemes for equations of thin film epitaxy*, Disc. Contin. Dyn. Sys. Ser. A, **28**, 405–423 (2010).
- [37] J. Shen, C. Wang, X. Wang and S. M. Wise, *Second-order convex splitting schemes for gradient flows with Ehrlich-Schwoebel type energy: application to thin film epitaxy*, SIAM J. Numer. Anal., **50**, 105–125 (2012).
- [38] Z. H. Qiao, C. Wang, S. M. Wise et al., *Error analysis of a finite difference scheme for the epitaxial thin film model with slope selection with an improved convergence constant*, Int. J. Numer. Anal. Model., **14**, 283–305 (2017).
- [39] Q. Cheng, J. Shen and X. F. Yang, *Highly efficient and accurate numerical schemes for the epitaxial thin film growth models by using the SAV approach*, J. Sci. Comput., **78**, 1467–1487 (2019).
- [40] W. B. Chen, S. Conde, C. Wang, X. M. Wang and S. M. Wise, *A linear energy stable scheme for a thin film model without slope selection*, J. Sci. Comput., **52**, 546–562 (2012).
- [41] Y. H. Xia, *A fully discrete stable discontinuous Galerkin method for the thin film epitaxy problem without slope selection*, J. Comput. Phys., **280**, 248–260 (2015).
- [42] L. L. Ju, X. Li, Z. H. Qiao and H. Zhang, *Energy stability and error estimates of exponential time differencing schemes for the epitaxial growth model without slope selection*, Math. Comput., **87**, 1859–1885 (2018).
- [43] J. Shin and H. G. Lee, *A linear, high-order, and unconditionally energy stable scheme for the epitaxial thin film growth model without slope selection*, Appl. Numer. Math., **163**, 30–42 (2021).
- [44] Z. H. Qiao, Z. R. Zhang and T. Tang, *An adaptive time-stepping strategy for the molecular beam epitaxy models*, SIAM J. Sci. Comput., **33**, 1395–1414 (2011).
- [45] H. L. Liao, X. H. Song, T. Tang and T. Zhou, *Analysis of the second-order BDF scheme with variable steps for the molecular beam epitaxial model without slope selection*, Sci. China-Math., **64**, 887–902 (2021).
- [46] H. L. Liao, B. Q. Ji, L. Wang and Z. M. Zhang, *Mesh-robustness of an energy stable BDF2 scheme with variable steps for the Cahn-Hilliard Model*, J. Sci. Comput., **92**, 52 (2022).
- [47] H. L. Liao, Z. Zhang, *Analysis of adaptive BDF2 scheme for diffusion equations*, Math. Comput., **90**, 1207–1226 (2021).
- [48] H. Gomez, T. Hughes, *Provably unconditionally stable, second-order time-accurate, mixed variational methods for phase-field models*, J. Comput. Phys., **230**, 5310–5327 (2011).